Effect of urea on micellar properties of aqueous solutions of nonionic surfactants

ARTICLE *in* THE JOURNAL OF PHYSICAL CHEMISTRY · OCTOBER 1991

Impact Factor: 2.78 · DOI: 10.1021/j100175a103

3 AUTHORS, INCLUDING:

Giuseppe Briganti
Sapienza University of Rome
58 PUBLICATIONS **811** CITATIONS
SEE PROFILE

Sudhakar Puvvada
Massachusetts Institute of Technology
23 PUBLICATIONS **1,113** CITATIONS
SEE PROFILE

plexation of Li^+ by the oligo(oxyethylene) side chains.

Conclusion

In summary, these results show that the electrochemical optical and electrooptical properties of PDHT films are strongly dependent on the nature and composition of the chemical environment of the polymer. PDHT exhibits a complex electrochemical behavior involving successive redox systems whose potential and magnitude depend on the composition of the electrolytic medium. Hydrophobic tetraalkylammonium cations have deleterious effects on the electrochemical response of PDHT and lead to an increase of the oxidation potential and a decrease of the doping level. In contrast, lithium cations produce an improvement of the definition of the voltammetric response, a decrease of the oxidation potential, and an increase of the overall electroactivity. These effects of lithium cations are observed also to a lesser extent in aqueous media in which PDHT remains highly electroactive. The electronic absorption spectrum of neutral PDHT shows a marked dependence on the composition of the electrolytic medium in which the film has been undoped, indicating that the effects observed in electrochemistry are at least partly due to a medium-induced control of the conformation of the conjugated backbone. Cyclic voltabsorptometry provides definitive evidence for conformational changes associated with distinct oxidation stages. These effects, which are particularly important in the presence of high concentrations of lithium cations, suggest that the complexation of lithium cations by the embryonic polyether side chains indirectly affects both the conformation and the rigidity of the conjugated poly(thiophene) backbone. Finally, the cyclic voltabsorptometric responses recorded at the maximum of the low-energy absorption band at 605 nm bring further support to the occurrence of electrochemically induced conformational relaxation and to an indirect control of the geometry and rigidity of the conjugated backbone through the complexation of lithium cations. Although further work is still required to fully elucidate the complex problem of the feed back effects of the interactions between the substituents and the chemical environment on the structure and properties of the conjugated backbone, these results, which confirm that PDHT represents the first step toward the design of ion-sensitive conjugated polymers, already have interesting implications for the development of sensors based on both the electrochemical and the optical properties of functional conjugated polymers.

Registry No. PDHT, 120245-40-1; CH_3CN, 75-05-8; Bu_4NClO_4, 1923-70-2; $LiClO_4$, 7791-03-9.

Effect of Urea on Micellar Properties of Aqueous Solutions of Nonionic Surfactants

G. Briganti,† S. Puvvada, and D. Blankschtein*

Department of Chemical Engineering and Center for Materials Science and Engineering, Massachusetts Institute of Technology, Cambridge, Massachusetts 02139 *(Received: April 15, 1991)*

We present results of a systematic experimental and theoretical investigation of the effect of urea on micellization, micellar growth, and phase separation of aqueous micellar solutions of the nonionic surfactant *n*-dodecyl hexaethylene oxide ($C_{12}E_6$). The experimental studies, which cover a wide range of urea concentrations from 0 to 6 M, involve determinations of the critical micellar concentration (cmc), micellar shape and size as a function of temperature, and liquid–liquid phase separation coexistence curves. We find that the addition of urea significantly affects micellar solution properties. In particular, (i) the cmc increases, (ii) micellar size decreases, (iii) the "sphere-to-rod" shape transition temperature shifts to higher values, and (iv) the critical point, associated with the coexistence curve, shifts to a higher temperature and concentration. We also find that the measured coexistence curves, at 0, 2, 4, and 6 M urea concentrations, collapse onto a single universal curve when plotted in reduced coordinates. In addition, we find that plots of the mean micellar hydrodynamic radius, R_h, vs $T_c - T$, where T_c is the critical temperature and T is the actual temperature, overlap for 0, 2, 4, and 6 M urea concentrations, with the resulting universal curve exhibiting a pronounced break at a value of $T_c - T \approx 37$ °C.

I. Introduction

Nonionic surfactants belonging to the alkyl polyethylene oxide family, typically abbreviated as C_iE_j, are widely used as detergents, solubilizers, and emulsifiers. Their practical importance has triggered a significant effort to gain a fundamental understanding of their micellization characteristics, as well as their phase behavior in both aqueous and nonaqueous media.[1]

The unique chemical structure of these surfactants offers a convenient model system to study how systematic variations in the hydrophobic/hydrophilic character of the surfactant affects micellar solution properties.[2] In particular, in aqueous solutions, the hydrophobic/hydrophilic character can be altered in a number of ways, which include (a) varying the number of methylene groups, i, or the number of ethylene oxide groups, *j*, of the surfactant, (b) varying the temperature of the solution, and (c) modifying the properties of the aqueous solvent.

A common method to modify the solvent consists of adding electrolytes, such as simple salts, or nonelectrolytes, such as urea. In particular, urea and its derivatives are well-known denaturants of proteins, and this has been attributed to the isothermal unfolding of the protein molecule (a change in conformation) due to weaker hydrophobic interactions in the presence of urea.[3] Several studies have been conducted to probe the effect of urea on the properties of aqueous micellar solutions.[4-6] Two different mechanisms for urea action have been proposed: (i) an indirect mechanism, whereby urea decreases the "structure" of water to facilitate the hydration of the nonpolar solute,[7,8] and (ii) a direct mechanism, whereby urea replaces some of the water molecules in the hy-

* To whom correspondence should be addressed.
† Permanent address: Dipartimento di Fisica, Universita di Roma "La Sapienza", Piazzale Aldo Moro, 00185 Rome, Italy.

(1) For a comprehensive survey on nonionic surfactants, including the alkyl polyethylene oxide family (C_iE_j), see: *Nonionic Surfactants*; Shick, M. J., Ed.; Arnold: London, 1967.
(2) Mitchell, D. J.; Tiddy, G. J. T.; Warring, L.; Bostock, T.; McDonald, M. P. *J. Chem. Soc., Faraday Trans. 1* **1983**, *79*, 975, and references cited therein.
(3) Tanford, C. *J. Am. Chem. Soc.* **1964**, *86*, 2050.
(4) Shick, M. J. *J. Phys. Chem.* **1964**, *68*, 3585.
(5) Emerson, M. F.; Holtzer, A. *J. Phys. Chem.* **1967**, *71*, 3320.
(6) Franks, F., Ed. *Water: A Comprehensive Treatise*; Plenum: New York, 1978; Vol. 4 and references cited therein.
(7) Wetlaufer, D. B.; Malik, S. K.; Stoller, L.; Coffin, R. L. *J. Am. Chem. Soc.* **1964**, *86*, 508.
(8) Franks, H. S.; Franks, F. *J. Chem. Phys.* **1968**, *48*, 4746.

0022-3654/91/2095-8989$02.50/0

dration shell of the solute.[9] The indirect mechanism has been widely accepted,[6] and many experimental results seem to support the hypothesis that urea acts as a "water-structure breaker". However, most of the experimental techniques used in these studies did not provide information at a molecular level, and conflicting interpretations of urea action have been proposed.[10] Recent computer simulations[11] as well as some studies using electron-spin resonance spectroscopy,[12] which have probed the system at a molecular level, seem to indicate that urea has a negligible effect on water structure and mainly replaces some water molecules in the hydration shell around the solute. These new findings appear to support the direct mechanism.

Since the properties of micellar solutions are determined by a delicate balance of hydrophobic/hydrophilic interactions of the surfactant with water,[13,14] one expects that urea may have a profound effect on these properties. Indeed, urea has been shown to (i) increase the critical micellar concentration (cmc) of ionic[15-17] and nonionic[18] surfactants, (ii) decrease the mean micellar hydrodynamic radius of ionic micelles,[19] and (iii) raise the cloud-point temperatures of aqueous solutions of nonionic surfactants[20] and lower the cloud-point temperatures of aqueous solutions of zwitterionic surfactants.[21] The observed effects were rationalized qualitatively in terms of the properties of urea–water solutions. For example, (i) the increase in the cmc was explained in terms of the enhanced solubility of the surfactant hydrophobic moiety in the presence of urea,[7,15-18] (ii) the reduction in the mean micellar hydrodynamic radius was attributed to a lowering of the interfacial tension between hydrocarbon and water in the presence of urea,[22] and (iii) the decrease in cloud-point temperatures of zwitterionic surfactants was rationalized by the fact that urea increases the dielectric constant of water.[21] However, a quantitative understanding of these effects remains a challenging unsolved problem.

Accordingly, the aim of the present work is twofold: (1) to conduct a systematic experimental study of the effect of urea on various micellar solution properties, such as (a) cmc, (b) micellar shape and size, and (c) phase separation behavior, in aqueous solutions of $C_{12}E_6$; (2) to provide a quantitative interpretation of the experimental results in the context of a recently developed molecular-thermodynamic theory of micellar solutions. We have chosen $C_{12}E_6$ because aqueous solutions of this nonionic surfactant offer a number of convenient experimental features which are described in section III.

The remainder of this paper is organized as follows. Section II describes the theoretical approach used to model the effect of urea on micellar properties of aqueous solutions of $C_{12}E_6$. Section III presents a description of the materials and experimental methods used to determine the various properties. Section IV discusses the estimation of the various molecular parameters which appear in the theoretical approach presented in section II. Section V compares the theoretical predictions with the experimental results and discusses possible mechanisms for the observed effect of urea. Finally, Section VI presents some concluding remarks.

II. Theoretical Approach

In this section we describe a recently developed molecular thermodynamic approach[23] to predict micellar solution properties. The new approach consists of blending a molecular model of micellization,[23] which captures the essential physicochemical forces operating at the micellar level, with a thermodynamic framework for micellar solutions,[24] which captures the salient features of the solution at the macroscopic level.

The theoretical formulation has been successfully utilized to predict micellar properties of aqueous solutions of nonionic surfactants, belonging to the alkyl polyethylene oxide and glucoside families, as a function of surfactant molecular architecture, surfactant concentration, and temperature.[23] The predicted properties, which compare favorably with available experimental data, include (i) cmc, (ii) micellar size distribution and its characteristics, (iii) micellar shape, (iv) coexistence curves, including the critical surfactant concentration, and (v) other thermodynamic properties such as the osmotic compressibility. The thermodynamic framework has also been successfully utilized to describe the phase behavior of aqueous solutions of zwitterionic surfactants, in the presence of added electrolytes[25] and urea,[21] over a wide range of surfactant concentrations and temperatures.

The encouraging results obtained so far have motivated us to implement the molecular-thermodynamic approach to describe the effect of urea on micellar properties of aqueous solutions of $C_{12}E_6$. Below, we present the modifications that need to be implemented in the molecular model of micellization to account for the presence of urea, as well as briefly describe the thermodynamic framework and the calculation of micellar solution properties. A complete account of the molecular-thermodynamic formulation can be found in ref 23.

A. Molecular Model of Micellization. The molecular model is used to estimate the magnitude of the free energy of micellization, $g_{mic}(n,l_c,sh)$, from the molecular characteristics of the surfactant and the solvent. Note that g_{mic} represents the free energy change when a surfactant molecule is transferred from bulk solvent (which includes water and any additives such as urea) to a micelle (characterized by an aggregation number, n, core-minor radius, l_c, and shape, sh) present in the same solvent. The numerical magnitude of g_{mic}, which reflects the propensity for micelles to form and subsequently grow, summarizes the many physicochemical forces responsible for micelle formation.

The free-energy contributions associated with the various forces are evaluated by using a thought process to "visualize" the formation of a micelle from individual monomers as a series of reversible steps. The free energy of micellization, g_{mic}, is then evaluated by summing the free-energy changes associated with each step of the thought process. Below, we describe the various steps of the thought process needed to estimate g_{mic} for the $C_{12}E_6$–water–urea system.

a. After the bond between the hydrophilic moiety ("head") and the hydrophobic moiety ("tail") of each $C_{12}E_6$ molecule is broken the tails are transferred from the urea–water (uw) solution to bulk hydrocarbon (hc). This gives rise to an attractive contribution, $g_{uw/hc}$, that can be conveniently evaluated by using a two-step transfer process. First, the tails are transferred from the urea–water solution to pure water (w). This gives rise to a repulsive contribution, $g_{uw/w}$, since urea enhances the solubility of the hydrocarbon tails in water. Subsequently, the tails are transferred

(9) Nozaki, Y.; Tanford, C. *J. Biol. Chem.* **1963**, *238*, 4074. Enea, O.; Jolicoeur, C. *J. Phys. Chem.* **1982**, *86*, 3370. Roseman, M.; Jencks, W. P. *J. Am. Chem. Soc.* **1975**, *97*, 631.

(10) Subramanian, S.; Sarma, T. S.; Balasubramanian, D.; Ahulawalia, J. C. *J. Phys. Chem.* **1971**, *75*, 815. Swenson, C. A. *Arch. Biochem. Biophys.* **1966**, *117*, 494.

(11) Kuharski, R. A.; Rossky, P. J. *J. Am. Chem. Soc.* **1984**, *106*, 5786. Kuharski, R. A.; Rossky, P. J. *J. Am. Chem. Soc.* **1984**, *106*, 5794.

(12) Baglioni, P.; Ferroni, E.; Kevan, L. *J. Phys. Chem.* **1990**, *94*, 4296.

(13) Tanford, C. *The Hydrophobic Effect*; Wiley: New York, 1980.

(14) Israelachvili, J. N. *Intermolecular and Surface Forces*; Academic: New York, 1985.

(15) Corkill, J. M.; Goodman, J. F.; Harrod, S. P.; Tate, J. R. *Trans. Faraday Soc.* **1967**, *63*, 2460.

(16) Das Gupta, P. K.; Moulik, S. P. *Colloid Polym. Sci.* **1989**, *267*, 246.

(17) Abu Hamdiyyah, M.; Al Mansour, L. *J. Phys. Chem.* **1979**, *83*, 2236.

(18) Shick, M. J. *J. Phys. Chem.* **1964**, *68*, 3585.

(19) Mazer, N. A.; Carey, M. C.; Kwasnick, R. F.; Benedek, G. B. *Biochemistry* **1979**, *18*, 3064.

(20) Han, S. K.; Lee, S. M.; Kim, M.; Schott, H. *J. Colloid Interface Sci.* **1989**, *132*, 444. Han, S. K.; Lee, S. M.; Schott, H. *J. Colloid Interface Sci.* **1988**, *126*, 393.

(21) Carvalho, B. L.; Briganti, G.; Chen, S.-H. *J. Phys. Chem.* **1989**, *93*, 4282.

(22) Missel, P. J.; Mazer, N. A.; Carey, M. C.; Benedek, G. B. In *Solution Behavior of Surfactants*; Mittal, K. L., Fendler, E. J., Eds.; Plenum: New York, 1982; Vol. 1, p 373.

(23) Puvvada, S.; Blankschtein, D. *J. Chem. Phys.* **1990**, *92*, 3710. Blankschtein, D.; Puvvada, S. *MRS Symp. Proc.* **1990**, *177*, 129. Puvvada, S.; Blankschtein, D. *Proceedings of the 8th International Symposium on Surfactants in Solution*; Mittal, K. L., Shah, D. O., Eds.; Plenum: New York, in press.

(24) Blankschtein, D.; Thurston, G. M.; Benedek, G. B. *Phys. Rev. Lett.* **1985**, *54*, 955. Blankschtein, D.; Thurston, G. M.; Benedek, G. B. *J. Chem. Phys.* **1986**, *85*, 7268.

(25) Huang, Y. X.; Thurston, G. M.; Blankschtein, D.; Benedek, G. B. *J. Chem. Phys.* **1990**, *92*, 1956.

from pure water to bulk hydrocarbon, which gives rise to an attractive contribution, $g_{w/hc}$. While $g_{w/hc}$ can be evaluated from the known solubilities of hydrocarbons in pure water,[26] the evaluation of $g_{uw/w}$ is more problematic because solubility data of *n*-alkanes in urea–water solutions are limited to those between methane and butane. To obtain a more accurate estimation of $g_{uw/w}$ for the longer tails, we have used the available solubility data for the shorter chains in conjunction with a recently proposed hydration shell hydrogen-bond model[27] (see section IV for more details). We find that $g_{uw/w} \approx (0.3\ U)\ kT$, where U is the molarity of urea, k is the Boltzmann constant, and T is the absolute temperature.

b. The next step involves the creation of an interface separating a hydrocarbon core (characterized by minor radius, l_c, and shape, sh) from the urea–water solution. This step reflects the repulsive interfacial contribution to g_{mic}, and the resulting free-energy change per monomer is evaluated by

$$g_\sigma = \sigma_0[1 - (S - 1)\delta/l_c](a - a_0) \quad (1)$$

where σ_0 is the interfacial tension between bulk hydrocarbon and the urea–water solution, δ is the Tolman distance (estimated[23] to be 2.25 Å for $C_{12}E_6$ and assumed to be independent of urea concentration), a_0 is the interfacial area screened from contact with water by the head, and $a = Sv/l_c$ is the total interfacial area per monomer which is exposed to water, where S is a shape factor (3 for spheres, 2 for cylinders, and 1 for disks or bilayers), and v is the volume of the tail (estimated[23] to be 323 Å^3). The dependence of σ_0 on urea concentration is given by $\sigma_0 = \sigma_0(U = 0) - \sigma_u U$, with $\sigma_u \approx 1.5$ dyn/cm (see section IV for details on the estimation procedure).

c. The next step involves estimating the free-energy change associated with the loss in conformational degrees of freedom of the tails inside the micellar core. This repulsive contribution, $g_{hc/mic}$, is calculated by utilizing a single-chain mean-field model.[28,29] This involves the generation of a large number of conformations of the tail inside the micellar core, in the context of the rotational isomeric state approximation, and the evaluation of the partition function and associated free energy. Note that this free-energy contribution is independent of urea concentration.

d. After the bond between the head and the tail is re-formed at the interface between the micellar core and the urea–water solution, the final step involves the evaluation of the free-energy change associated with steric interactions between the uncharged surfactant heads. This repulsive contribution, g_{st}, is calculated by treating the heads present at the interface as an ideal localized monolayer, which reflects the fact that each head is physically attached to a tail at the interface. The resulting free-energy contribution is given by

$$g_{st} = -kT \ln (1 - (a_h/a)) \quad (2)$$

where a_h is the average cross-sectional area of the head. This important molecular characteristic reflects the interactions of the ethylene oxide head with the urea–water solution and consequently is expected to vary both with temperature and with the concentration of urea (for details on the estimation of these variations see section IV).

The four contributions, $g_{uw/hc}$, g_σ, $g_{hc/mic}$, and g_{st}, to g_{mic} are calculated for the three regular shapes of spheres, infinite-sized cylinders, and infinite-sized disks as a function of the micellar core minor radius, l_c. The total free energy, $g_{mic}(l_c, sh)$, is then minimized with respect to l_c to obtain the optimum values of the micellar core-minor radius, $l^*_c(sh)$, and the free energy of micellization, $g^*_{mic}(sh)$, for that shape. Subsequently, the optimum shape of the micelle, sh*, is determined by minimizing $g^*_{mic}(sh)$ with respect to sh. This procedure allows us to predict whether the micelles that form exhibit two-dimensional, one-dimensional, or no growth. However, since entropic considerations limit the size of micelles, g_{mic} for the intermediate nonregular finite-sized micelles needs to be estimated. This is done by linearly interpolating between the optimum free energies corresponding to the limiting regular shapes. For example, g_{mic} for a micelle that exhibits one-dimensional growth is estimated by linearly interpolating between the free energies of micellization of an infinite-sized cylindrical micelle and a finite-sized spherical micelle. For additional details see ref 23.

B. Thermodynamic Framework. It is well established that over the range of urea concentrations of interest in this work (0–6 M), urea mixes ideally with water.[30] Therefore, we expect urea to distribute uniformly in the solution. There is also evidence that when a urea–water micellar solution undergoes liquid–liquid phase separation, the urea concentrations in the two coexisting phases do not differ significantly.[21] This seems to suggest that, as a first approximation, it is reasonable to treat the ternary system $C_{12}E_6$–water–urea as a pseudobinary system of $C_{12}E_6$ in an effective solvent, whose properties depend on the concentration of urea.

With this in mind, we use a thermodynamic description of the micellar solution which incorporates the following features: (i) the free energy of micellization, g_{mic}; (ii) a distribution of micelles in chemical equilibrium with each other; (iii) the entropy of mixing micelles, monomers, and solvent; and (iv) a mean-field interaction potential between the micelles. The total Gibbs free energy of the solution, G, is given by[23,24]

$$G = N_w\mu^0_w + N_s\mu^0_1 + \sum_n nN_n g_{mic}(n, l_c, sh) + kT(N_w \ln X_w + \sum_n N_n \ln X_n) - \tfrac{1}{2}CN_s\phi \quad (3)$$

where N_n and N_w are the number of *n*-mers and solvent molecules, respectively, X_n and X_w are the corresponding mole fractions, N_s is the total number of surfactant molecules, ϕ is the total surfactant volume fraction, μ^0_1 and μ^0_w are the standard-state chemical potentials of surfactant and solvent, respectively, and C is a mean-field interaction parameter that reflects the magnitude of the effective intermicellar attraction.

Using the free-energy expression given in eq 3 and imposing the conditions of chemical equilibria between micelles having different aggregation numbers, the following expression for the micellar size distribution, $\{X_n\}$, can be obtained[23,24]

$$X_n = ((X_1 e)^n/e)e^{-\beta n g_{mic}(n)} \quad (4)$$

where X_1 is the monomer mole fraction and $\beta = 1/kT$. All equilibrium properties associated with the distribution, including the cmc and characteristics of the distribution, can be computed by solving eq 4 in conjunction with the material balance equation, $X = \sum nX_n$, where X is the total surfactant mole fraction.

In particular, we have evaluated the cmc by plotting the monomer mole fraction, X_1, as a function of the total surfactant mole fraction, X, and identifying the concentration where the plot exhibits a break.

We have also computed[24] the relative variance, V, of the micellar size distribution

$$V = \langle (n - \langle n \rangle_w)^2 \rangle_w / \langle n \rangle_w^2 \quad (5)$$

where $\langle n \rangle_w$ is the weight-average micellar aggregation number. Note that the relative variance reflects the polydispersity and shape of the micelles.

The critical point, which signals the onset of phase separation, is characterized by the critical surfactant concentration, X_c, and the critical temperature, T_c. At the critical point, thermodynamic stability requires that the two conditions, $(\partial^2 g/\partial X^2)_{T,P} = 0$ and $(\partial^3 g/\partial X^3)_{T,P} = 0$ should be satisfied, where $g = G/(N_w + N_s)$. By simultaneously solving these two equations, we have evaluated

(26) Abraham, M. H. *J. Chem. Soc., Faraday Trans. 1* **1984**, *80*, 153.
(27) Muller, N. *J. Phys. Chem.* **1990**, *94*, 3856. Muller, N. *Acc. Chem. Res.* **1990**, *23*, 23.
(28) Ben-Shaul, A.; Szleifer, I.; Gelbart, W. M. *J. Chem. Phys.* **1985**, *83*, 3597. Szleifer, I.; Ben-Shaul, A.; Gelbart, W. M. *J. Chem. Phys.* **1985**, *83*, 3612.
(29) Gruen, D. W. R. *J. Phys. Chem.* **1985**, *89*, 146, 153.
(30) Stokes, R. H. *Aust. J. Chem.* **1967**, *20*, 2087. Grant, E. H.; Keefe, S. K.; Shack, R. *Adv. Mol. Relax. Processes* **1972**, *4*, 217.

the values of X_c and of the critical interaction parameter, C_c, corresponding to the value of C at T_c.

In addition, the entire cloud-point (coexistence) curve can be calculated by demanding the simultaneous equalities of the monomer and solvent chemical potentials in the two coexisting phases. For additional details see ref 23.

III. Materials and Experimental Methods

We have chosen $C_{12}E_6$ because aqueous solutions of this nonionic surfactant offer a number of convenient experimental features: (i) the cmc is very low (6.7×10^{-5} M), thus providing a broad dilute concentration range to study micellar solution properties in the absence of significant intermicellar interactions; (ii) the solution exhibits a cloud-point (coexistence) curve with a lower consolute (critical) temperature of $T_c \approx 51$ °C, thus allowing a convenient temperature range over which the phase separation behavior can be studied as a function of urea concentration under atmospheric pressure; and (iii) the micelles in this system exhibit a sphere-to-rod shape transition as the temperature is increased beyond approximately 18 °C, and this temperature is sufficiently below the critical temperature so that shape transitions can be studied by using light scattering measurements without the complicating influence of critical fluctuations.

A. Materials and Sample Preparation. Homogeneous $C_{12}E_6$ was obtained from Nikko Chemicals, Tokyo (Lot 7008), and used without any further purification. The high purity of the surfactant was confirmed by the absence of any detectable minimum in the measured surface tension vs surfactant concentration curves, as well as by comparing our measured value of $T_c \approx 51.14$ °C for the $C_{12}E_6$–water system with values reported in the literature from highly purified samples[31] In addition, to ensure uniformity in the results, all our measurements were conducted by using the same lot of surfactant. Urea was obtained from Merck with a nominal purity of 99.5% and was used without any further purification. All solutions were prepared using deionized water which had been fed through a Milli-Q ion-exchange system.

B. Critical Micellar Concentration Measurement. The critical micellar concentration (cmc) was obtained by the surface tension method. This method is based on the fact that the surface tension decreases quite rapidly with increasing surfactant concentration until the cmc, above which it remains practically constant. The measured surface tension was plotted as a function of the logarithm of the surfactant concentration, and the cmc was estimated from the break in the resulting surface tension curve. A Wilhelmy plate tensiometer (Kruss K10T) was used to measure the surface tensions. All measurements were carried out in a thermostated device maintained at 25 °C.

C. Coexistence Curve Determination. Coexistence curves for liquid–liquid phase separation were determined according to the cloud-point method.[21,25] In the case of $C_{12}E_6$ in water, this method consists of visually identifying the temperature at which solutions of known concentration become cloudy when the temperature is raised. Each sample was placed in a transparent thermoregulated device whose temperature was controlled to within 0.01 °C. Initially, each sample was cooled to a temperature low enough so that it exhibited a single, clear, homogeneous phase. The temperature was then raised in small steps until the solution started to cloud at a temperature T_u. As soon as clouding was observed, the temperature was lowered in small steps until the cloudiness disappeared at a temperature T_d. T_{cloud} was then determined by taking the average of T_u and T_d. Note that at each step the sample was first stirred thoroughly, with a magnetic stirrer, to ensure temperature homogeneity and subsequently observed for any signs of cloudiness with the stirrer shut off. The entire procedure was repeated several times with smaller steps in temperature. This cycling procedure was adopted to ensure reproducibility and reversibility in the observed clouding behavior. All measurements were reproducible to within 0.05 °C.

D. Light Scattering Measurements. Dynamic light scattering and intensity measurements were performed by using a He–Ne laser (λ = 6328 Å) in a 90° configuration and a home-made correlator with 128 channels. These measurements were performed as a function of temperature (5–65 °C) and urea concentration (0, 2, 4, and 6 M urea) at a fixed surfactant mole fraction of 10^{-3}. At this surfactant concentration both intensity and scattering correlation functions have been shown[32] to be independent of scattering angle in $C_{12}E_6$–D_2O solutions. The dynamic light scattering data were interpreted by using a cumulants analysis.[33] The mean micellar hydrodynamic radius was calculated, in the context of the Stokes–Einstein relation, from the first cumulant by using available[34] viscosity data for urea–water solutions.

IV. Estimation of Molecular Parameters

As discussed in section II, the molecular thermodynamic approach can be used to predict various properties of micellar solutions by using molecular information about the surfactant and the solvent. The important molecular parameters involved, including the effect of urea on them, are described below.

In section IIA we saw that the solubility of the surfactant tail in the solvent is an important molecular parameter which needs to be adequately described. Indeed, the increased solubility of the tail in water in the presence of urea is captured by the free-energy contribution, $g_{uw/w}$. Recall that this contribution represents the free-energy change associated with transferring the tail from the urea–water solution to pure water. Since solubility data of *n*-alkanes in urea–water solutions are only available for those between methane and butane,[7] the required extrapolation to the longer tail of $C_{12}E_6$ seems questionable. We have therefore estimated this contribution using a recently proposed[27] hydration shell hydrogen-bond model. This is a two-state model, where the hydrogen atom of a water molecule is either hydrogen-bonded or not, and the average fraction of broken and intact hydrogen bonds is calculated through a knowledge of the bond-breaking enthalpies and entropies (the adjustable parameters of the model). Using this simple model, it was possible to reproduce measured values of excess heat capacities, enthalpies, entropies, and free energies of transfer from pure hydrocarbon to aqueous solutions with and without added urea. The model could also explain the very puzzling trends in water proton NMR chemical shifts for solutions of polar molecules with large hydrophobic groups. Using this model and a cavity surface area of 530 Å^2 for the C_{12} tail, we estimate a value of approximately $0.3kT$ per molar urea for the free-energy change, $g_{uw/w}$. Note that a value of 530 Å^2 for the cavity surface area of a C_{12} chain was obtained by extrapolating the values reported[35] for shorter (up to C_{10}) *n*-alkanes.

A second important molecular feature is the value of the interfacial tension between bulk hydrocarbon and the urea–water solution, σ_0. In this respect, interfacial tensions between heptane and water in the presence of 1 and 2 M urea were recently measured.[36] The measured values indicate that in the presence of urea σ_0 is lowered by approximately 1.5 dyn/cm per molar urea. This value was linearly extrapolated up to 6 M urea and used in all our calculations. Note that the linear extrapolation is reasonable since, as mentioned earlier, urea–water solutions exhibit ideal behavior over this range of urea concentrations.[30]

The third important molecular characteristic of the surfactant is the average cross-sectional area of the head, a_h. Indeed, the magnitude of a_h determines the value of the steric contribution, g_{st}, to the free energy of micellization. As stated in section I, the hydrophobic/hydrophilic character of the surfactant can be altered

(31) Strey, R.; Pakusch, A. In *Surfactants in Solution*; Mittal, K. L., Bothorel, P., Eds.; Plenum: New York, 1986; Vol. 4, p 465. Fujimatsu, H.; Ogasawara, S.; Kuroiwa, S. *Colloid Polym. Sci.* **1988**, *266*, 594.

(32) Brown, W.; Rymden, R. *J. Phys. Chem.* **1987**, *60*, 775.

(33) Koppel, D. E. *J. Chem. Phys.* **1972**, *57*, 4814. Mazer, N. A.; Benedek, G. B.; Carey, M. C. *J. Phys. Chem.* **1976**, *80*, 1075.

(34) Venkatesan, V. K.; Suryanarayana, C. V. *J. Phys. Chem.* **1956**, *60*, 775.

(35) Amidon, G. L.; Yalkowsky, S. H.; Anik, S. T.; Valvani, S. C. *J. Phys. Chem.* **1975**, *79*, 2239.

(36) Gabrielli, G. Personal communication.

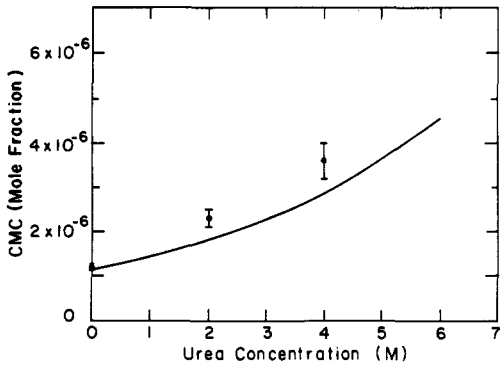

Figure 1. Measured critical micellar concentration (cmc) of aqueous solutions of $C_{12}E_6$ for 0, 2, and 4 M urea concentrations. The solid line represents the theoretical prediction.

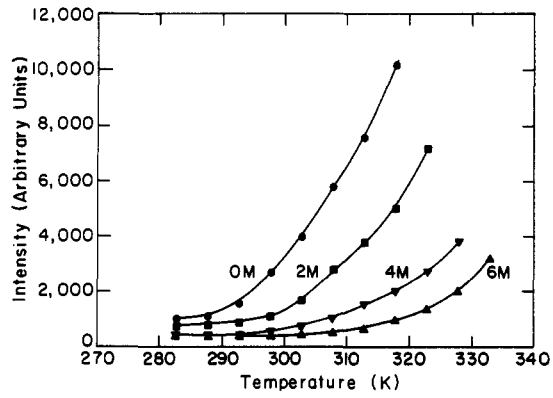

Figure 2. Measured intensity of scattered light (in arbitrary units) as a function of temperature for 0, 2, 4, and 6 M urea concentrations. The various symbols represent experimental points. The solid lines are drawn to guide the eye.

by varying temperature. Thus, when temperature is increased, $C_{12}E_6$ becomes less hydrophilic.[37] The precise mechanism leading to the observed temperature dependence is still a topic of active research.[38] One explanation which has been suggested[2,37] is that the ethylene oxide groups of $C_{12}E_6$ hydrate in the presence of water, with the hydration number decreasing with increasing temperature. Consequently, we expect a_h to decrease as the temperature is increased. In addition, according to the direct mechanism[9] described in section I, urea perturbs the hydration shell of the head by replacing some of the water molecules. Since a urea molecule is approximately 2.5 times larger than a water molecule, we expect a_h to increase with the addition of urea at a fixed temperature. Note that the larger size of the urea molecules also implies that a_h will decrease at a faster rate with increasing temperature in the presence of urea. These qualitative arguments are summarized by the following empirical expression for the dependence of a_h on temperature and urea concentration

$$a_h = a_{h0}\{1 - H(T - 298)\} \quad (6)$$

with $a_{h0} = (38.1 + 0.8U)$ Å^2 and $H = (7.5 + 0.57U) \times 10^{-3}$/°C, where U is the molarity of urea. Note that the values of a_{h0} and H at 0 M urea are the same as those used to predict the properties of $C_{12}E_6$ in pure water.[23] The values used to describe the dependence of a_{h0} and H on urea concentration have been adjusted to best-fit experimental results. Work is currently in progress to validate these numbers by using other independent measurements.

Below, we use the molecular-thermodynamic theory described in section II, with the three molecular parameters estimated in this section, to predict and interpret a broad spectrum of micellar solution properties as a function of urea concentration and temperature.

V. Results and Discussions

Figure 1 shows predictions of the cmc of aqueous solutions of $C_{12}E_6$ as a function of urea concentration at 25 °C. The predicted values are in good agreement with our measured values at 0, 2, and 4 M urea concentrations. The estimated experimental uncertainties, shown by the error bars, reflect the error in determining the cmc from the measured surface tension curve. Note that as the concentration of urea was increased, the measured surface tension values were more scattered, and as a result the cmc could only be determined with a larger uncertainty. Measurements could not be performed at 6 M urea because of the precipitation of a white solid, presumably urea or a urea complex, on the Wilhelmy plate and on the sides of the sample container. The observed increase in the cmc with increasing urea concentration is consistent with the enhanced solubility of the nonpolar tail and the increased hydration of the ethylene oxide (EO) head in the presence of urea. In the context of the molecular model of micellization, we find that the enhanced solubility of the tail in urea–water solutions is the dominant factor in determining the cmc.

Figure 2 shows the measured intensity of scattered light (in arbitrary units) as a function of temperature for 0, 2, 4, and 6 M urea concentrations at a fixed surfactant mole fraction of 10^{-3}. The figure clearly indicates that, at fixed urea concentration, the scattering intensity remains approximately constant up to a certain temperature T^* (T^* = 15, 22, 28, and 37 °C for 0, 2, 4, and 6 M urea concentrations, respectively), beyond which it increases rapidly. In each case, T^* is sufficiently below the critical temperature ($T_c - T^* \approx 37$ °C) that critical fluctuation effects should be minimal. Consequently, it is reasonable to associate the increase in intensity with an increase in micellar size. With this in mind, the picture that seems to emerge is one in which, for $T < T^*$, the micelles are relatively small with their size approximately constant, and for $T > T^*$, the micelles exhibit growth. In addition, urea is seen to have a significant effect on T^*, shifting it to higher values. These conclusions are supported by the measured values of the mean micellar hydrodynamic radius, R_h, as a function of temperature and urea concentration reported in Figure 4 (see discussion below). The observed experimental trends can be rationalized in terms of interactions between the ethylene oxide (EO) heads and water in the presence of urea. As described in section IV, the EO heads of $C_{12}E_6$ dehydrate with increasing temperature. This reduces the value of a_h and associated steric repulsions between the heads, thus enabling the micelles to grow from spheroidal structures (characterized by a larger curvature) into rodlike structures (characterized by a smaller curvature) as temperature is increased. However, addition of urea at fixed temperature increases the value of a_h, thus effectively increasing steric repulsions. This, in turn, implies smaller micelles and a shift in the sphere-to-rod transition temperature, T^*, to higher values.

The postulated sphere-to-rod transition occurring at T^*, as well as the shift in T^* to higher temperatures when urea is added, can be predicted in the context of the molecular-thermodynamic theory. For this purpose, it is convenient to consider the relative variance of the micellar size distribution, V, which constitutes a measure of polydispersity and micellar shape. In particular,[23] small monodisperse spheroidal micelles are characterized by $V = 0$, whereas large polydisperse rodlike micelles are characterized by $V = 0.5$. We have therefore used eq 5 to predict the temperature variation of V (at a fixed surfactant mole fraction of 10^{-3}) for 0, 2, 4, and 6 M urea concentrations (see Figure 3). The figure shows that there is a narrow temperature range in which micelles grow from small monodisperse spheroidal micelles ($V = 0$) to large polydisperse rodlike micelles ($V = 0.5$) and that this transition temperature is shifted to higher values with increasing urea concentration. The theoretical predictions of the transition temperatures are in very good agreement with the experimentally determined T^* values shown by arrows in Figure 3, obtained from the break in the intensity vs temperature curves shown in Figure 2.

Figure 4 shows the measured mean micellar hydrodynamic radius, R_h, as a function of temperature for 0, 2, 4, and 6 M urea

(37) Nilsson, P. G.; Lindman, B. *J. Phys. Chem.* **1983**, *87*, 4756.
(38) Kjellander, R.; Florin, E. *J. Chem. Soc., Faraday Trans. 1* **1981**, *77*, 2053. Goldstein, R. E. *J. Phys. Chem.* **1984**, *80*, 5340. Karlstrom, G. *J. Phys. Chem.* **1985**, *89*, 4962.

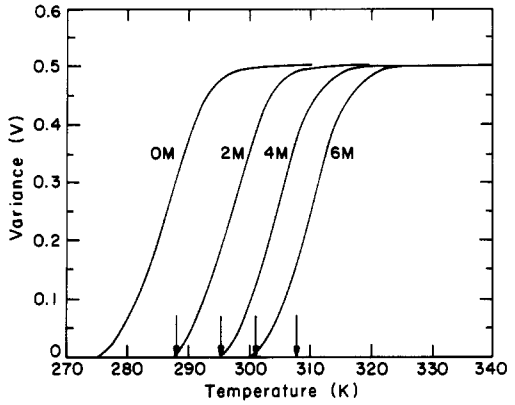

Figure 3. Predicted variance (V) of the micellar size distribution as a function of temperature for aqueous solutions of $C_{12}E_6$ at 0, 2, 4, and 6 M urea concentrations. The theoretical predictions were made at a surfactant mole fraction of 10^{-3}. The arrows represent the experimentally determined sphere-to-rod shape transition temperatures obtained from the break in the intensity vs temperature curves shown in Figure 2.

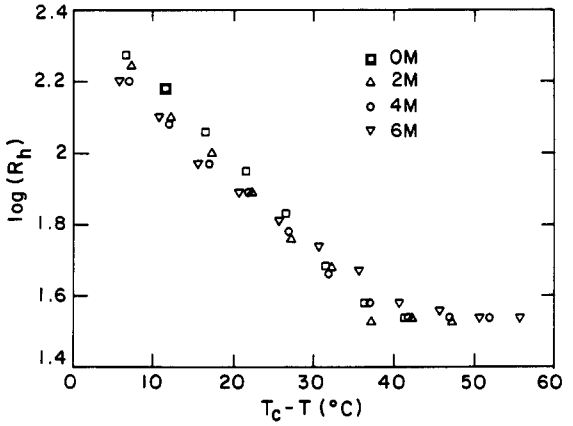

Figure 4. Measured mean micellar hydrodynamic radius, R_h, as a function of $T_c - T$ for aqueous solutions of $C_{12}E_6$ at 0, 2, 4, and 6 M urea concentrations. The resulting universal curve exhibits a break at a value of $T_c - T \approx 37$ °C.

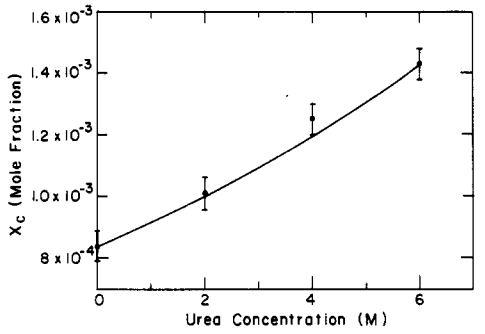

Figure 5. Measured critical concentration for phase separation, X_c, of aqueous solutions of $C_{12}E_6$ for 0, 2, 4, and 6 M urea concentrations. The solid line represents the theoretical prediction.

concentrations. Note that the results are presented as log (R_h) vs $T_c - T$, the difference between the critical temperature, T_c, and the actual temperature, T. We have used this representation to illustrate the rather remarkable fact that the curves for all urea concentrations overlap and that the behavior of R_h exhibits a pronounced change at a value of $T_c - T \approx 37$ °C for all urea concentrations. This behavior seems to suggest a strong correlation between micellar shape and size and phase separation. We will comment further on this correlation after discussing the effect of urea on phase separation (see below).

Figure 5 shows the predicted variation of the critical concentration for phase separation, X_c, as a function of urea concentration. For these predictions, we have used the measured values of T_c in conjunction with the molecular-thermodynamic theory.

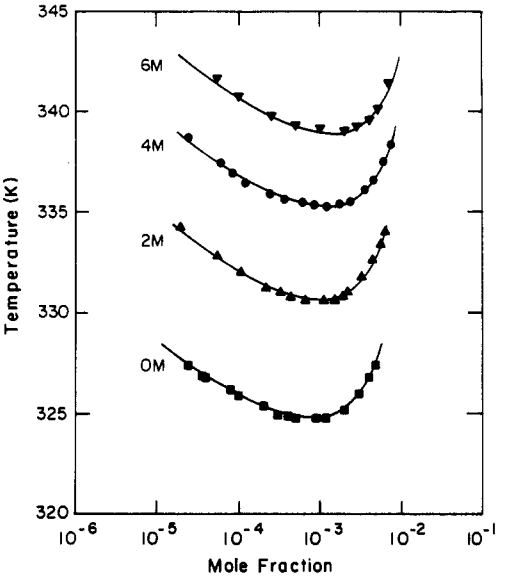

Figure 6. Measured cloud-point temperatures (various symbols) for 0, 2, 4, and 6 M urea concentrations. The solid lines are drawn to guide the eye.

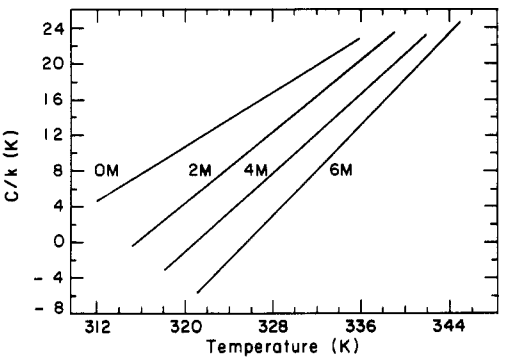

Figure 7. Calculated values (solid lines) of the effective intermicellar attraction parameter, C, as a function of temperature for 0, 2, 4, and 6 M urea concentrations.

The predicted values are in excellent agreement with our experimental values at 0, 2, 4, and 6 M urea concentrations. Note that the experimental critical concentration values were determined from the minima of the measured cloud-point curves. The estimated experimental uncertainties, shown by the error bars, reflect the error in determining the minima.

Figure 6 shows the measured cloud-point temperatures (various symbols) for 0, 2, 4, and 6 M urea concentrations (the solid lines are drawn to guide the eye). Using the measured values, in the context of the molecular-thermodynamic theory, it is possible to evaluate the effective mean-field intermicellar attraction parameter, C, as a function of temperature and urea concentration. Figure 7 shows that, at a fixed temperature, the effective intermicellar attraction, captured by C, decreases with increasing urea concentration. Furthermore, the value of C increases linearly with temperature with the slope, dC/dT, increasing with increasing urea concentration. This dependence of C on temperature and urea concentration can be rationalized in terms of competing attractive van der Waals and repulsive steric interactions between the hydrated micelles.[2,14] Indeed, if one envisions that the addition of urea results in a thicker hydration layer (because urea is larger than water, and according to the direct mechanism it replaces some of the water molecules in the hydration layer of the micelle), steric repulsions between micelles would increase in the presence of urea at a fixed temperature. Furthermore, since urea increases the static dielectric constant of water,[30] the strength of the attractive van der Waals interactions would also increase in the presence of urea at a fixed temperature. However, since the overall effect of adding urea is a reduction in the effective intermicellar attraction parameter, C, it appears that urea has a larger effect on

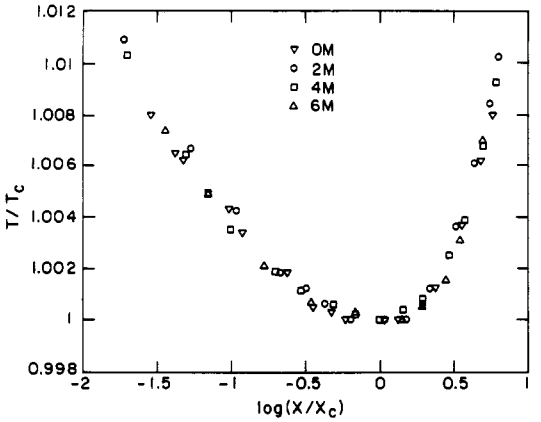

Figure 8. Experimental cloud-point curves (from Figure 6) plotted in reduced coordinates, T/T_c, and, X/X_c, where T_c and X_c are the critical temperature and concentration, respectively. The collapse onto a single universal curve is apparent.

the steric repulsions than on the van der Waals attractions between the hydrated micelles. Similarly, as temperature is increased at fixed urea concentration, the dehydration of the EO heads (giving rise to a thinner hydration layer) will decrease steric repulsions between the hydrated micelles, thus contributing to an increase in the value of C. Since the EO head dehydrates at a faster rate in the presence of urea (see section IV) and the temperature dependence of the van der Waals attraction is independent of urea concentration (because the change in the dielectric constant of water in the presence of urea is weakly dependent on temperature[30]), dC/dT would increase with increasing urea concentration.

We return next to the possible correlation between micellar shape and size and phase separation suggested by the data in Figure 4. It is tempting to speculate that the link between these two features is provided by the hydration characteristics of the EO heads. Indeed, this determines (1) the magnitude of a_h, which controls the magnitude of intramicellar steric repulsions and is primarily responsible for the evolution in micellar shape and size with increasing temperature and urea concentration, and (2) the magnitude of C, through changes in intermicellar steric repulsions, responsible for changes in phase separation characteristics, such as T_c, with urea concentration.

Finally, Figure 8 shows the experimental cloud-point (coexistence) curves plotted in reduced coordinates, T/T_c, and, X/X_c, where T_c and X_c are the critical temperature and concentration, respectively. It is apparent that all the experimental points, corresponding to 0, 2, 4, and 6 M urea concentrations, collapse onto a single universal curve. Further work is needed to understand the origin of this very interesting phenomenon.

VI. Conclusions

The data presented in this paper clearly show that urea has a significant effect on the properties of aqueous micellar solutions of $C_{12}E_6$. In particular, we find that the addition of urea (i) increases the value of the cmc, (ii) decreases the micellar size, (iii) shifts the sphere-to-rod transition temperature to higher values, and (iv) shifts the critical point, associated with the coexistence curve, to a higher temperature and concentration. A very interesting observation is that the coexistence curves, at 0, 2, 4, and 6 M urea concentrations, collapse onto a single universal curve when plotted in reduced coordinates. A similar behavior is observed for plots of the mean micellar hydrodynamic radius, R_h, vs temperature at 0, 2, 4, and 6 M urea concentrations. In addition, we have shown that it is possible to quantitatively rationalize these effects in the context of the molecular-thermodynamic theory.

A number of important issues need further clarification and development. In particular, the hydration characteristics of the ethylene oxide headgroups seems to play a very important role in the determination of the magnitudes of both the intermicellar and intramicellar steric repulsions, through C and a_h, respectively. An understanding of the microscopic origin of hydration, including its dependence on the concentration of urea and temperature, can provide a link between the inter- and intramicellar repulsions. A microscopic description of hydration could also facilitate the description of the origin of the observed collapses of the various coexistence curves and R_h onto single universal curves.

Acknowledgment. This research was supported in part by a National Science Foundation (NSF) Presidential Young Investigator (PYI) Award to D.B. and NSF Grant DMR-84-18718 administered by the Center for Materials Science and Engineering at MIT. D.B. is grateful for the support of the Texaco–Mangelsdorf Career Development Professorship at MIT. He is also grateful to the following companies for providing PYI matching funds: BASF, British Petroleum America, Exxon, Kodak, Texaco, and Unilever. G.B. acknowledges partial support from Eniricerche, Italy.

Registry No. $C_{12}E_6$, 3055-96-7; urea, 57-13-6.